



HAL
open science

INVESTIGATION ON THE STABILITY IN A THICK SPRAY MODEL

Victor Fournet

► **To cite this version:**

Victor Fournet. INVESTIGATION ON THE STABILITY IN A THICK SPRAY MODEL. 2024.
hal-04586793

HAL Id: hal-04586793

<https://hal.science/hal-04586793>

Preprint submitted on 24 May 2024

HAL is a multi-disciplinary open access archive for the deposit and dissemination of scientific research documents, whether they are published or not. The documents may come from teaching and research institutions in France or abroad, or from public or private research centers.

L'archive ouverte pluridisciplinaire **HAL**, est destinée au dépôt et à la diffusion de documents scientifiques de niveau recherche, publiés ou non, émanant des établissements d'enseignement et de recherche français ou étrangers, des laboratoires publics ou privés.

INVESTIGATION ON THE STABILITY IN A THICK SPRAY MODEL

VICTOR FOURNET¹

Abstract. The aim of this work is to discuss linear stability and instability properties of a thick spray model. We linearize the equation and we give a criterion on the equilibrium to have linear instability. We also present numerical illustrations.

Résumé. Le but de cet article est de discuter des propriétés de stabilité et d'instabilité linéaire d'un modèle de spray épais. Nous linéarisons les équations et nous donnons un critère sur l'équilibre pour avoir instabilité linéaire. Nous présentons aussi des illustrations numériques.

1. INTRODUCTION

The aim of this paper is to discuss linear stability properties of a multiphase model that characterizes suspensions of particles in an underlying gas, commonly referred to as a "spray" [15]. A typical system describing such spray can be expressed as follows [1, 6, 32]:

$$\begin{cases} \partial_t f + \mathbf{v} \cdot \nabla_x f + \nabla_v \cdot (\mathbf{\Gamma} f) = 0 \\ \partial_t(\alpha \varrho) + \nabla_x \cdot (\alpha \varrho \mathbf{u}) = 0 \\ \partial_t(\alpha \varrho \mathbf{u}) + \nabla_x \cdot (\alpha \varrho \mathbf{u} \otimes \mathbf{u}) + \alpha \nabla_x p(\varrho) = D_\star \int_{\mathbf{R}^3} (\mathbf{v} - \mathbf{u}) f, dv. \end{cases} \quad (1)$$

In system (1), the first equation is a Vlasov-type equation, describing particle evolution through a distribution function $f = f(t, \mathbf{x}, \mathbf{v}) \geq 0$ in the phase space $\mathbf{T}^3 \times \mathbf{R}^3$ for times $t > 0$. The second and third equations are the barotropic compressible Euler equations, governing the evolution of density $\varrho = \varrho(t, \mathbf{x}) \geq 0$ and velocity $\mathbf{u} = \mathbf{u}(t, \mathbf{x}) \in \mathbf{R}^3$ of the fluid for times $t > 0$ and positions $\mathbf{x} \in \mathbf{T}^3$. This system characterizes the "thick" spray regime, where the total volume occupied by particles is significant compared to the fluid volume, leading to coupling between the fluid and particles.

The volume fraction of the fluid, denoted as $\alpha = \alpha(t, \mathbf{x})$, is a key parameter, related to f through the formula $\alpha(t, \mathbf{x}) = 1 - \frac{4}{3} \pi r_p^3 \int_{\mathbf{R}^3} f(t, \mathbf{x}, \mathbf{v}) dv$. Here, we assume $\alpha(t, \mathbf{x}) \in [0, 1]$, which differs from the "thin" spray regime where this quantity is close to 1 and absent from the equations [4]. The particle radius $r_p > 0$ is a constant, and the force field $\mathbf{\Gamma} = \mathbf{\Gamma}(t, \mathbf{x}, \mathbf{v})$ acting on particles is given by

$$\mathbf{\Gamma}(t, \mathbf{x}, \mathbf{v}) = -\nabla_x p(\varrho) - \frac{D_\star}{\frac{4}{3} \pi r_p^3} (\mathbf{v} - \mathbf{u}).$$

This force comprises two terms: the term $\frac{D_\star}{\frac{4}{3} \pi r_p^3} (\mathbf{v} - \mathbf{u})$ represents a drag force exerted on the particles by the fluid. The feedback of the drag force on the fluid is present in the third equation of (1), denoted as the

¹ Laboratoire Jacques Louis Lions, Sorbonne Université, 4 place Jussieu, 75005 Paris, France and CEA, DAM, DIF, F-91297, Arpajon, France, victor.fournet@sorbonne-universite.fr

”Brinkman force.” The drag coefficient $D_\star \geq 0$ is typically provided in semi-empirical forms. The term $-\nabla_x p(\varrho)$ is specific to thick spray. Its presence is consistent with the fact that the system (1) is formally linked to bifluid equation [16], where there is a common pressure gradient to both phases.

In contrast with the thin spray equations for which there exists a rich litterature on the subject (see [2, 4, 7, 18, 24, 30] and the references therein), the mathematical litterature on thick spray is much more limited and only a few results are available [6, 30]. Indeed, the presence of both the pressure gradient $-\nabla_x p$ in the Vlasov equation and of the volume fraction α in the fluid equations make the rigorous study of thick spray equations challenging. We refer to [9, 17, 20] for recent rigorous works on thick sprays.

This model is applicable to diverse physical phenomena at various length scales, including medical aerosols [7, 8], combustion in engines [1], atmospheric aerosols [29], and astrophysics for modeling gas giants and exoplanets [21].

The friction force is usually considered as a leading effect in fluid-particles flows. However, in this study we take for mathematical convenience $D_\star = 0$ because the linearized equation can then be rewritten using the framework of Lax and Kato [26, 28] (the reader interested by preliminary results concerning the more physical case $D_\star > 0$ can refer to the last section of [10]). The resulting model is expressed as

$$\begin{cases} \partial_t f + \mathbf{v} \cdot \nabla_x f - \nabla_x p(\varrho) \cdot \nabla_v f = 0 \\ \partial_t(\alpha \varrho) + \nabla_x \cdot (\alpha \varrho \mathbf{u}) = 0 \\ \partial_t(\alpha \varrho \mathbf{u}) + \nabla_x \cdot (\alpha \varrho \mathbf{u} \otimes \mathbf{u}) + \alpha \nabla_x p(\varrho) = 0. \end{cases} \quad (2)$$

2. LINEAR STABILITY

2.1. Linearisation of thick spray equations

We consider the following homogeneous solution of (2)

$$\begin{cases} \varrho(t, \mathbf{x}) = \varrho_0 > 0, \\ \mathbf{u}(t, \mathbf{x}) = 0, \\ f(t, \mathbf{x}, \mathbf{v}) = f_0(\mathbf{v}) \end{cases}$$

where the density $n_0 = \int_{\mathbf{R}^3} f_0 \, dv$ is related to the volume fraction α_0 by

$$1 - \frac{4}{3} \pi r_p^3 n_0 = \alpha_0 \in (0, 1). \quad (3)$$

Following [9], we perform the linearization

$$\begin{cases} \varrho(t, \mathbf{x}) = \varrho_0 + \varepsilon \varrho_1(t, \mathbf{x}) + O(\varepsilon^2) \\ \mathbf{u}(t, \mathbf{x}) = \varepsilon \mathbf{u}_1(t, \mathbf{x}) + O(\varepsilon^2) \\ f(t, \mathbf{x}, \mathbf{v}) = f_0(\mathbf{v}) + \varepsilon \sqrt{f_0(\mathbf{v})} f_1(t, \mathbf{x}, \mathbf{v}) + O(\varepsilon^2). \end{cases}$$

Dropping the quadratic terms and the subscripts, one obtains [9] the following linear thick spray equations with $\tau(t, \mathbf{x}) = -\varrho_1(t, \mathbf{x})/\varrho_0^2$ and $c_0 = \sqrt{p'(\varrho_0)}$

$$\begin{cases} \alpha_0 \varrho_0 \partial_t \tau = \alpha_0 \nabla_x \cdot \mathbf{u} + m_\star \nabla_x \cdot \int_{\mathbf{R}^3} \mathbf{v} \sqrt{f_0} f \, dv \\ \alpha_0 \varrho_0 \partial_t \mathbf{u} = \alpha_0 \varrho_0^2 c_0^2 \nabla_x \tau \\ \partial_t f + \mathbf{v} \cdot \nabla_x f + \varrho_0^2 c_0^2 \nabla_x \tau \cdot \frac{\nabla_v f_0}{\sqrt{f_0}} = 0. \end{cases} \quad (4)$$

In the rest of this work, we set the constants to 1.

To study the linear stability of (4), we introduce the following operator

$$iH = \begin{pmatrix} 0 & \nabla_x \cdot \nabla_x \cdot \int \mathbf{v} \sqrt{f_0(\mathbf{v})} \cdot d\mathbf{v} \\ \nabla_x & 0 \\ -\frac{\nabla_v f_0}{\sqrt{f_0}} \cdot \nabla_x & 0 & -\mathbf{v} \cdot \nabla_x \end{pmatrix} \quad (5)$$

So that (4) rewrites

$$U'(t) = iHU(t)$$

with $U = (\tau, \mathbf{u}, f)$.

2.2. Spectral analysis

2.2.1. Instabilities of the linear problem

We look for exponentially growing modes of (4), i.e. solutions of the form

$$f(t, x, v) = \alpha(v)e^{-i\omega t}e^{ikx}, \quad \tau(t, x) = \beta e^{-i\omega t}e^{ikx}, \quad u(t, x) = \gamma e^{-i\omega t}e^{ikx}, \quad (6)$$

with $k \in \mathbf{Z}$, $\omega \in \mathbf{C}$ with $\Im m(\omega) > 0$, $\alpha \in L^\infty(\mathbf{R})$, β and $\gamma \in \mathbf{R}$. Injecting this ansatz into (4), one gets

$$\begin{cases} -i\omega\beta = ik\gamma + i \int kv\sqrt{f_0(v)}\alpha(v) dv \\ -i\omega\gamma = ik\beta \\ (-i\omega + ikv)\alpha(v) = -i\beta \frac{kf'_0(v)}{\sqrt{f_0(v)}} \end{cases}$$

Then one obtains

$$\alpha(v) = \frac{-\beta k}{-\omega + kv} \frac{f'_0(v)}{\sqrt{f_0(v)}}, \quad \gamma = -\frac{\beta}{\omega} k, \quad (7)$$

and

$$-i\omega\beta = -ik^2 \frac{\beta}{\omega} - i\beta \int \frac{k^2 v \partial_v f_0(v)}{kv - \omega} dv.$$

In particular, one has the dispersion relation

$$\frac{k^2}{\omega^2} + \int \frac{f'_0(v)}{v - \omega/k} dv = 1. \quad (8)$$

Conversevely, if (8) holds for some $k \in \mathbf{Z}$ and $\omega \in \mathbf{C}$ with $\Im m(\omega) > 0$, then the modes (6) with α and γ given by (7) are solutions of (4). We proved the following proposition

Proposition 2.1. *The linearized equations (4) have exponentially growing modes if and only if there exists $k \in \mathbf{Z}$ and $\omega \in \mathbf{C}$ with $\Im m(\omega) > 0$ satisfying (8). In that case, α and γ are given by (7) for any $\beta \in \mathbf{R}$.*

This situation is similar to the case of the Vlasov-Poisson system [12, 31, 35]

$$\begin{cases} \partial_t f + \mathbf{v} \cdot \nabla_x f - \nabla_x \varphi \cdot \nabla_v f = 0 \\ -\Delta_x \varphi = \int_{\mathbf{R}} f dv - 1. \end{cases} \quad (9)$$

as observed by Penrose [33]. Applying the same strategy to the linearized Vlasov-Poisson equations, one finds the dispersion relation

$$Z\left(\frac{\omega}{k}\right) := \int \frac{f'_0(v)}{v - \omega/k} dv = k^2 \quad (10)$$

Now, denoting \mathfrak{S}_+ the upper half plane, a solution $\omega(k)$ of (10) exists if and only if $Z(\mathfrak{S}_+)$ contains a positive real number k^2 . The set $Z(\mathfrak{S}_+)$ is bounded and its boundary is the curve

$$x \mapsto PV \int \frac{f'_0(v)}{v - x} dv + i\pi f'_0(x)$$

and this curve is bounded, starting and ending at the origin, and for k large enough, the equation (10) has no solution. Therefore, in the case where the profile f_0 leads to a solution $\omega \in \mathfrak{S}_+$ of (10), there is a finite number of exponentially growing modes. For the system (4), the situation is quite different since the equation (8) can be rewritten as

$$\zeta(z) := \frac{1}{z^2} + \int \frac{f'_0(v)}{v - z} dv = 1, \quad z \in \mathbf{C},$$

with $z = \omega/k$. Therefore, if $z = \omega/k \in \mathfrak{S}_+$ is a solution, then so is $z = (n\omega)/(kn)$, with $n \in \mathbf{N}^*$. This situation also happens in other singular kinetic equations such as the Vlasov-Benney equation (see [5])

$$\begin{cases} \partial_t f + v\partial_x f - \partial_x V \partial_v f = 0 \\ V = \int_{\mathbf{R}} f dv, \end{cases} \quad (11)$$

for which the dispersion relation writes

$$\int \frac{f'_0(v)}{v - \omega/k} dv = 1,$$

or this equation, which can be seen as a kinetic version of the incompressible Euler equation (see [3, 23])

$$\begin{cases} \partial_t f + v\partial_x f - \partial_x V \partial_v f = 0 \\ \int_{\mathbf{R}} f dv = 1. \end{cases} \quad (12)$$

for which the dispersion relation writes

$$\int \frac{f'_0(v)}{v - \omega/k} dv = 0,$$

However, because of the term $\frac{1}{z^2}$, the set $\zeta(\mathfrak{S}_+)$ is unbounded, and the curve

$$x \mapsto \frac{1}{x^2} + PV \int \frac{f'_0(v)}{v - x} dv + i\pi f'_0(x), \quad x \in \mathbf{R},$$

is also unbounded. Nevertheless, we expect that distribution f_0 with multiples bumps (corresponding to so-called "two-stream instability" of plasma physics [11, 19]) is an unstable profile (as shown in the numerical simulations below).

2.2.2. The maxwellian case

In the maxwellian case $f_0(v) = e^{-v^2/2}$, the operator H defined by (5) restricted to $X := L_0^2(\mathbf{T}) \times L_0^2(\mathbf{T}) \times L_0^2(\mathbf{T} \times \mathbf{R})$ with domain $D[H] = \{U \in X, HU \in X\}$ is self-adjoint, so the dispersion relation (8) has no solution $\Im m(\omega) > 0$. Moreover its spectrums can be decomposed in terms of theory of measure [26, 28]. It yields the following decomposition

$$X = X^{\text{ac}} \oplus X^{\text{sc}} \oplus X^{\text{pp}}.$$

where X^{ac} (resp. X^{sc} , resp. X^{pp}) corresponds to the absolutely continuous (resp. singular continuous, resp. pure point) part of the spectrum. The pure point subspace X^{pp} is spanned by the eigenvectors

$$X^{\text{pp}} = \text{Span}\{\varphi \in X, H\varphi = \lambda\varphi \text{ for some } \lambda \in \mathbf{R}\}.$$

On the other hand, the subspace X^{ac} is characterized [22, 25, 34] by the existence of a dense subset $A \subset X^{\text{ac}}$ such that

$$\varphi \in A \Rightarrow \left\| (H - \lambda - i\varepsilon)^{-1} \varphi \right\|_X = O\left(\frac{1}{\sqrt{\varepsilon}}\right). \quad (13)$$

This characterisation is known as the Christensen criterion. Applying this criterion to the operator H , one finds that the space X can be decomposed as $X = X^{\text{ac}}$, it is then a classical fact of scattering theory [26, 28] that, denoting e^{itH} the semi-group associated with H , the solution $U(t) = (\tau(t), u(t), f(t)) = e^{itH}(\tau_{\text{ini}}, u_{\text{ini}}, f_{\text{ini}})$ weakly converges to 0 in X as $t \rightarrow \infty$. Then it is possible to show that $\tau(t)$ and $u(t)$ strongly converges in L^2_0 to 0 as $t \rightarrow \infty$, using the conservation of the quadratic norm. It yields the following result [10].

Theorem 2.2. *If $f_0(v) = e^{-v^2/2}$, the operator H is self-adjoint and one has the decomposition $X = X^{\text{ac}}$. As a consequence, a solution $(\tau(t, \cdot), \mathbf{u}(t, \cdot), f(t, \cdot, \cdot))$ of (4) weakly converges in X to 0 as $t \rightarrow \infty$. One also has convergence of the acoustic energy $\|\tau(t)\|_{L^2}^2 + \|\mathbf{u}(t)\|_{L^2}^2$ to 0 at $t \rightarrow +\infty$.*

The strategy to prove Theorem 2.2 is similar to the one used in [13, 14] to prove a linear Landau damping for the Vlasov-Poisson system. This fact and the numerical simulations (see Figure 3 below) leads to believe that this result is qualitatively similar to the linear Landau damping. In [9], the authors prove a linear stability result around radially decreasing profiles of the form

$$f_0(v) = F\left(\frac{v^2}{2}\right)$$

where $F : \mathbf{R}_+ \rightarrow \mathbf{R}_+$ is a smooth strictly decreasing function, the maxwellian case corresponds to $F(w) = e^{-w}$. It is expected that Theorem 2.2 is also true in this case. We also refer to the last section of [10] for preliminary results on the reintroduction of a nonzero friction $D_\star > 0$ in the system and its consequences on the damping effect, using formal computations and numerical simulations.

3. EXAMPLES

In this section, we show examples of stable and unstable equilibrium f_0 . The numerical illustrations are done by discretizing the nonlinear equations (2) with the methods described in [10]. For the initial conditions, we take

$$\begin{cases} \varrho(t=0, x) = \varrho_0 \\ u(t=0, x) = 0 \\ f(t=0, x, v) = (1 + \varepsilon \cos(kx))f_0(v). \end{cases}$$

with $\varrho_0 = 1$, $k = 0.5$ and $\varepsilon = 0.001$.

3.1. Damping

In this section, we consider the case where

$$f_0(v) = \frac{1}{\sqrt{2\pi}} e^{-v^2/2}.$$

This case has been studied in [10]. In this case the dispersion relation (8) has no roots $\omega(k)$ with positive imaginary part, and thus, no growing modes exists. A plot of the evolution of $\|\varrho - \varrho_0\|_{L^2}(t)$ and $\|u\|_{L^2}(t)$ in

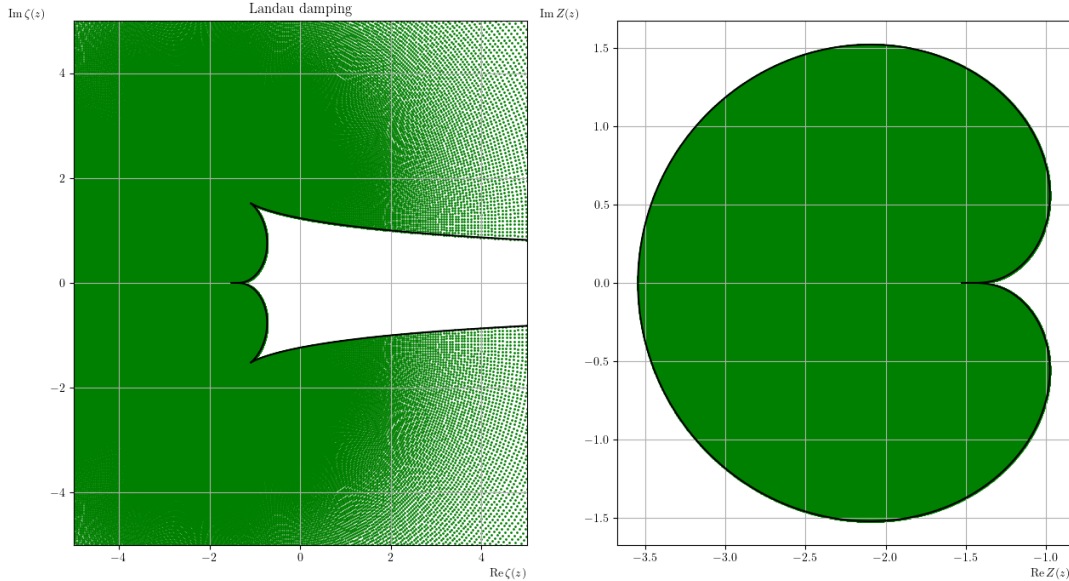


FIGURE 1. Plot of the functions $\zeta(s)$ (left) and $Z(s)$ in the case where $f_0(v) = (\sqrt{2\pi})^{-1} e^{-v^2/2}$. The image of the upper half complex plane is in green, and the image of the real line is the black curve. Notice how 1 is not in the image of ζ .

time can be found in Figure 3. One observes that these quantities decrease exponentially, so the acoustic energy which is the sum of these quantities decreases as well as predicted by Theorem 2.2. A possible strategy to predict the rate of decay observed in the numerical simulation is to follow Landau [27] and to formally apply a Fourier-Laplace transform on the linear system (4). The complete computations can be found in [10].

The dispersion relation are illustrated in Figure 1 for Vlasov-Poisson and the system (4). The image of \Im_+ are represented by the green dots for ζ on the left and for Z on the right. The black curve is the image of \mathbf{R} under ζ and Z . One sees the boundedness of $Z(\Im_+)$, and the fact that there is no positive real number in $Z(\Im_+)$. Observe that the situation is quite different for ζ , indeed the set $\zeta(\Im_+)$ appears to be unbounded, the same is true for the curve $\zeta(\mathbf{R})$. The curve is actually closed at infinity since $f'_0(0) = 0$.

3.2. Two-stream instability

We consider here a case where f_0 writes

$$f_0(v) = \frac{1}{2\sqrt{2\pi}} \left(e^{-\frac{(v-v_0)^2}{2}} + e^{-\frac{(v+v_0)^2}{2}} \right), \quad v_0 = 2.5.$$

By analogy with plasma physics [11, 19], we call this test "two-stream instability". The evolution of $\|\varrho - \varrho_0\|_{L^2}$ and $\|u\|_{L^2}$ in time is plotted in Figure 4e. One observes that at first, the quantities $\|\varrho - \varrho_0\|_{L^2}$ and $\|u\|_{L^2}$ increase exponentially, as predicted by the linear theory. At some later time saturation sets in and the solution enters the nonlinear regime. In Figure 4a, one can see the apparition of vortex in the phase space distribution, eventually the streams merge and there is a significant filamentation of the phase space distribution. The nature of this problem makes it a challenging numerical problem. As all modes are growing, the saturation time decreases when the mesh is refined, because the scheme is able to capture higher modes.

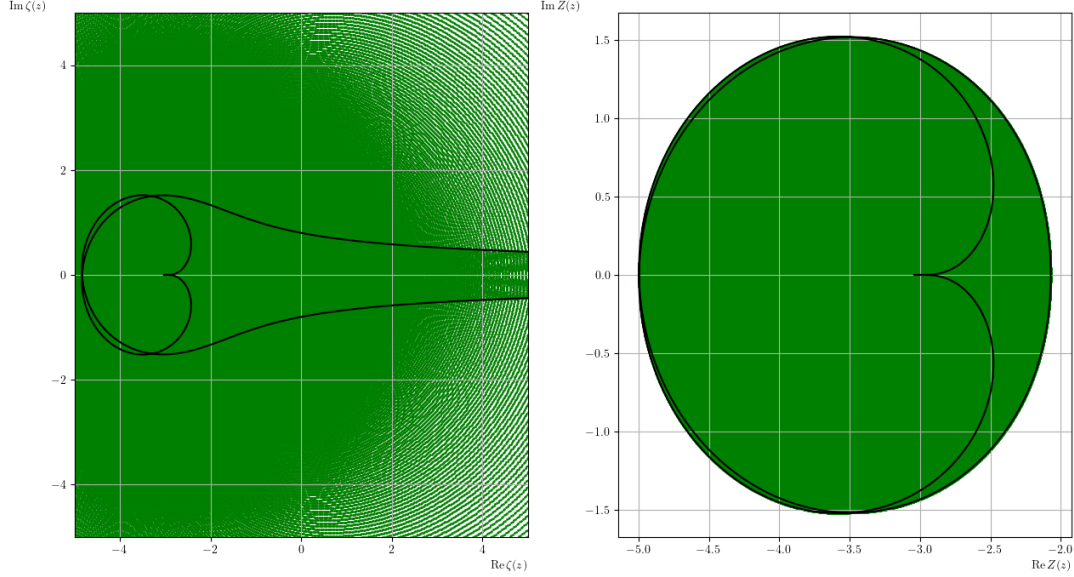


FIGURE 2. Plot of the functions $\zeta(s)$ (left) and $Z(s)$ in the case where $f_0(v) = (2\sqrt{2\pi})^{-1} \left(e^{-(v-v_0)^2/2} + e^{-(v+v_0)^2/2} \right)$ with $v_0 = 2.5$. The image of the upper half complex plane is in green, and the image of the real line is the black curve. Notice how 1 is in the image of ζ .

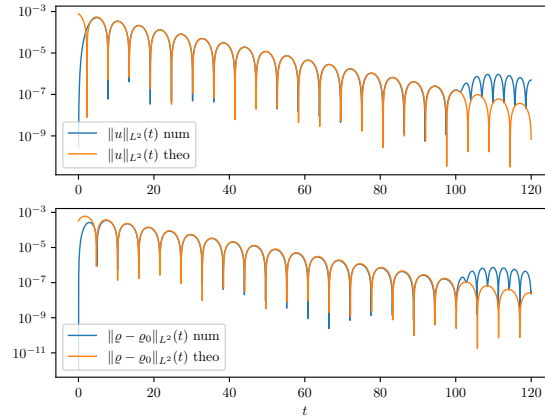
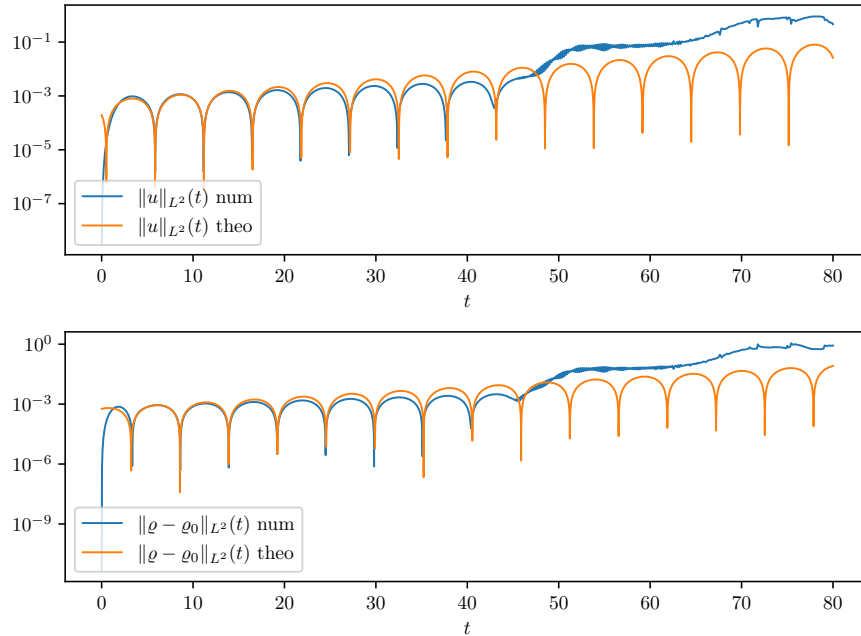
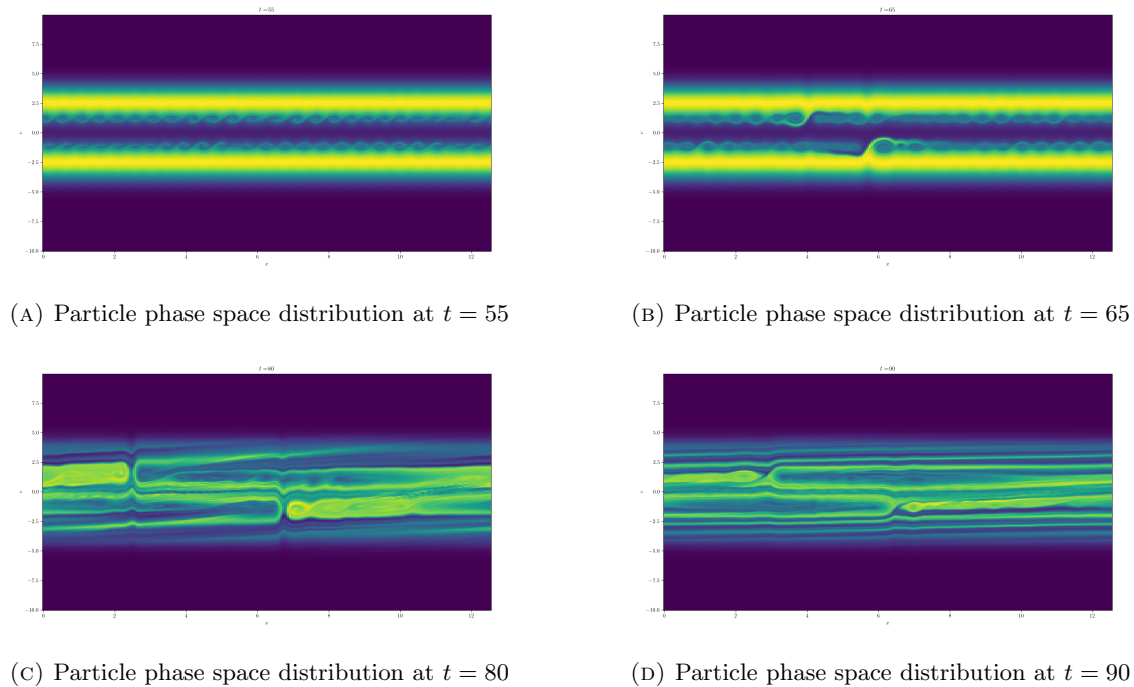


FIGURE 3. Plot of the damping of the L^2 norm of $\varrho - \varrho_0$ and u . In blue, the numerical solution. In orange, the solution predicted by the linear theory.

The dispersion relation is illustrated in Figure 2 for Vlasov-Poisson and the system (4). It appears that the set $\zeta(\mathfrak{S}_+)$ is the whole complex plane.



(E) Plot of the L^2 norm of $q - q_0$ and u . In blue, the numerical solution. In orange, the solution predicted by the linear theory.

FIGURE 4. Two-stream instability

REFERENCES

- [1] A. A. Amsden, P. J. O'Rourke, and T. D. Butler. Kiva-ii: A computer program for chemically reactive flows with sprays. Technical report, Los Alamos National Lab. (LANL), Los Alamos, NM (United States), 1989.
- [2] O. Anoshchenko and A. Boutet de Monvel-Berthier. The existence of the global generalized solution of the system of equations describing suspension motion. *Mathematical Models and Methods in Applied Sciences*, 1997.
- [3] A. Baradat. Nonlinear instability in vlasov type equations around rough velocity profiles. *Annales de l'Institut Henri Poincaré C, Analyse non linéaire*, 2020.
- [4] C. Baranger and L. Desvillettes. Coupling euler and vlasov equations in the context of sprays: The local-in-time, classical solutions. *Journal of Hyperbolic Differential Equations*, 03(01):1–26, 2006.
- [5] C. Bardos and A. Nouri. A vlasov equation with dirac potential used in fusion plasmas. *Journal of Mathematical Physics*, 2012.
- [6] L. Boudin, L. Desvillettes, and R. Motte. A modeling of compressible droplets in a fluid. *Communications in Mathematical Sciences*, 1:657–669, 2003.
- [7] L. Boudin, C. Grandmont, B. Grec, S. Martin, A. Mecherbet, and F. Noël. Fluid-kinetic modelling for respiratory aerosols with variable size and temperature. In *CEMRACS 2018 – Numerical and mathematical modeling for biological and medical applications: deterministic, probabilistic and statistical descriptions*, volume 67, pages 100–119. EDP Sci., Les Ulis, 2020.
- [8] L. Boudin, C. Grandmont, A. Lorz, and A. Moussa. Modelling and numerics for respiratory aerosols. *Communications in Computational Physics*, 18(3):723–756, 2018.
- [9] C. Buet, B. Després, and L. Desvillettes. Linear stability of thick sprays equations. *Journal of Statistical Physics*, 190(53), 01 2023.
- [10] C. Buet, B. Després, and V. Fournet. Analog of Linear Landau Damping in a coupled Vlasov-Euler system for thick sprays. <https://hal.science/hal-04265990>, hal-04265990. Submitted, Oct. 2023.
- [11] N. Crouseilles, T. Respaud, and E. Sonnendrücker. A forward semi-lagrangian method for the numerical solution of the vlasov equation. *Computer Physics Communications*, 180(10):1730–1745, 2009.
- [12] P. Degond. Spectral theory of the linearized vlasov-poisson equation. *Transactions of the American Mathematical Society*, 376(5), 1986.
- [13] B. Després. Scattering structure and landau damping for linearized vlasov equations with inhomogeneous boltzmannian states. *Annales de l'Institut Henri Poincaré*, 2019.
- [14] B. Després. Trace class properties of the non homogeneous linear vlasov–poisson equation in dimension 1+1. *Journal of Spectral Theory*, 11(2):709–742, 2021.
- [15] L. Desvillettes. Some aspects of the modelling at different scales of multiphase flows. *Computer methods in applied mechanics and engineering*, 2010.
- [16] L. Desvillettes and J. Mathiaud. Some aspects of the asymptotics leading from gas-particles equations towards multiphase flows equations. *Journal of Statistical Physics*, 141, 2010.
- [17] L. Ertzbischoff and D. Han-Kwan. On well-posedness for thick spray equations. Arxiv, March 2023.
- [18] L. Ertzbischoff, D. Han-Kwan, and A. Moussa. Concentration versus absorption for the vlasov-navier-stokes system on bounded domains. *Nonlinearity*, 2021.
- [19] F. Filbet and T. Xion. Conservative discontinuous galerkin/hermite spectral method for the vlasov–poisson system. *Communications on Applied Mathematics and Computation*, 4:34–59, 2020.
- [20] V. Fournet, C. Buet, and B. Després. Local-in-time existence of strong solutions to an averaged thick sprays model. *Kinetic and Related Models*, 0(0):0–0, 2023.
- [21] P. Gao, H. R. Wakeford, S. E. Moran, and V. Parmentier. Aerosols in exoplanet atmospheres. *Journal of Geophysical Research: Planets*, 126(4), 2021.
- [22] K. Gustafson and G. Johnson. On the absolutely continuous subspace of a self-adjoint operator. *Helvetica Physica Acta*, 47(2):163–166, 1976.
- [23] D. Han-Kwan and M. Hauray. Stability issues in the quasineutral limit of the one-dimensional vlasov–poisson equation. *Communications in Mathematical Physics*, 2014.
- [24] D. Han-Kwan, A. Moussa, and I. Moyano. Large time behavior of the vlasov-navier-stokes system on the torus. *Archive for Rational Mechanics and Analysis*, 2020.
- [25] T. Kato. Wave operators and unitary equivalence. *Pacific Journal of Mathematics*, 15(1), 1965.
- [26] T. Kato. *Perturbation Theory for Linear Operators*. Springer, 1995.
- [27] L. Landau. On the vibration of the electronic plasma. *Journal of Physics*, 10(1):25–34, 1946.
- [28] P. D. Lax. *Functional Analysis*. Wiley, 2014.
- [29] T. Mather, D. Pyle, and C. Oppenheimer. Tropospheric volcanic aerosol. *Washington DC American Geophysical Union Geophysical Monograph Series*, 139, 2003.
- [30] J. Mathiaud. Local smooth solutions of a thin spray model with collisions. *Mathematical Models and Methods in Applied Sciences*, (20):191–221, 2010.
- [31] C. Mouhot and C. Villani. On landau damping. *Acta Mathematica*, 207(1), 2011.

- [32] P. J. O'Rourke. Collective drop effects on vaporizing liquid sprays. Technical report, Los Alamos National Lab., 1981.
- [33] O. Penrose. Electrostatic instabilities of a uniform non-maxwellian plasma. *Physics of Fluids*, 1960.
- [34] M. Reed and B. Simon. *Analysis of Operators*, volume 4. Elsevier, 1978.
- [35] T. H. Stix. *The Theory of Plasma Waves*. New York et al.: McGraw-Hill Book Co., 1962.